NAVAL POSTGRADUATE SCHOOL
Monterey, California

THESIS

IDENTIFICATION OF PUSH-TO-TALK TRANSMITTERS USING WAVELETS AND SPECTRAL CORRELATION

by

Abdulla Mufarrah Abdulla

September 1996

Thesis Advisor: Ralph Hippenstiel
Co-Advisor: Monique P. Fargues

REPORT DOCUMENTATION PAGE

Form Approved
OMB No. 0704-0188

1. AGENCY USE ONLY (Leave blank)	2. REPORT DATE	3. REPORT TYPE AND DATES COVERED
	September 1996	Master's Thesis

4. TITLE AND SUBTITLE
Identification of Push-to-Talk Transmitters Using Wavelets and Spectral Correlation

5. FUNDING NUMBERS

6. AUTHOR(S)
Abdulla Mufarrah Abdulla

7. PERFORMING ORGANIZATION NAME(S) AND ADDRESS(ES)
Naval Postgraduate School
Monterey, California 93943

8. PERFORMING ORGANIZATION REPORT NUMBER

9. SPONSORING/MONITORING AGENCY NAME(S) AND ADDRESS(ES)

10. SPONSORING/MONITORING AGENCY REPORT NUMBER

11. SUPPLEMENTARY NOTES
The views expressed in this thesis are those of the author and do not reflect the official policy or position of the Department of Defense or the U.S. Government.

12a. DISTRIBUTION/AVAILABILITY STATEMENT
Approved for public release; distribution is unlimited.

12b. DISTRIBUTION CODE

13. ABSTRACT (Maximum 200 words)

The purpose of this thesis is to find an automated way to identify push-to-talk transmitters using a wavelet or a spectral correlation based approach. In the wavelet approach, a distance algorithm is applied to the wavelet scales of the signal and the template. One signal from each transmitter set is taken as a template. The distance algorithm computes the distance between the local extrema of the wavelet coefficients of the template and the signal. Results show that the Wavelet Transform (WT) distance algorithm is able to classify the four signal sets accurately. Good identification results are achieved even at low signal-to-nose ratios. In the spectral correlation approach an averaged template for each signal is used. The spectral coefficients for templates and signals are computed by extracting the magnitude squared of the Fast Fourier Transform (FFT) of the data. This method performs better for most signals better than the wavelet method because it can identify at lower signal to noise levels than the wavelet method does.

14. SUBJECT TERMS	15. NUMBER OF PAGES
wavelet analysis, classification/identification, spectral correlation, push-to-talk transmitters	57
	16. PRICE CODE

17. SECURITY CLASSIFICATION OF REPORT	18. SECURITY CLASSIFICATION OF REPORT	19. SECURITY CLASSIFICATION OF ABSTRACT	20. LIMITATION OF ABSTRACT
UNCLASSIFIED	UNCLASSIFIED	UNCLASSIFIED	UL

Approved for public release; distribution is unlimited

IDENTIFICATION OF PUSH-TO-TALK TRANSMITTERS USING WAVELETS AND SPECTRAL CORRELATION

Abdulla Muffarrah Abdulla
Captain, Bahrain Army
B.S. Electrical Engineering, Northrop University, 1987

Submitted in partial fulfillment of the
requirements for the degree of

MASTER OF SCIENCE IN ELECTRICAL ENGINEERING

from the

NAVAL POSTGRADUATE SCHOOL

September 1996

ABSTRACT

The purpose of this thesis is to find an automated way to identify push-to-talk transmitters using a wavelet or a spectral correlation based approach. In the Wavelet approach, a distance algorithm is applied to the wavelet scales of the signal and the template. One signal from each transmitter signal set is taken as a template. The distance algorithm computes the distance between the local extrema of the wavelet coefficients of the template and the signal. Results show that the Wavelet Transform (WT) distance algorithm is able to classify the four signal sets accurately. Good identification results are achieved even at low signal-to-noise ratios. In the spectral correlation approach an averaged template for each signal set is used. The spectral coefficients for templates and signals are computed by extracting the magnitude squared of the Fast Fourier Transform (FFT) of the data. This method performs better for most signals than the wavelet method because it can identify at lower signal to noise levels than the wavelet method does.

TABLE OF CONTENTS

ACKNOWLEDGEMENTS

I would like to thank my thesis advisor, Professor Ralph Hippenstiel, for his assistance and making this thesis work possible. Also, I would like to thank Professor Monique Fargues for her assistance as my co-adviser.

A grateful thanks to LCDR Nabil Khalil a Ph.D. candidate from the Eqyptian Army for his assistance during my studies at the Naval Postgraduate School.

I. INTRODUCTION

Some characteristics of signals generated by a transmitter are believed to be unique to a given transmitter. The transient response is defined as the change in carrier strength from the off-state to the on-state, and vice versa. The turn-on response (from the off-state to the on-state) is unique for every transmitter, regardless of its make or model. By analyzing the turn-on response we can map a given intercepted signal to a particular transmitter. Therefore, if we can reliably extract the unique parameters of the turn-on transient, then we can identify a given transmitter.

Time-frequency analysis of stationary signals is a well-researched subject. This type of analysis uses the Fourier Transform (FT) method which is appropriate for stationary signals. However, since the FT method uses a complex exponential basis function that exists over infinite time, we cannot use the FT method for non-stationary signals. In 1946, Gabor [1] introduced the sliding time window (Gaussian) to gain time information from the FT method. This modified FT method is called the Short-Time Fourier Transform (STFT). It uses a modulated complex exponential as a basis function and processes only the windowed data segment. This method, however, requires the signal to be stationary within these small portions, otherwise it will have limitations in reflecting the time-evolution of frequencies within the window.

The Wavelet Transform (WT) method is a more suitable technique for transient signal analysis than the STFT method in the sense that it provides more conclusive information regarding time evolution. Basis functions of the WT, unlike the FT, have a very short duration and are nonzero only for that short duration. This compact support makes the WT localized in frequency and time. Moreover, if we use wavelets we can choose the particular wavelet function from a large number of compactly supported wavelets that can be used as orthogonal basis functions.

Spectral correlation analysis provides a useful tool for the classification of transient signals (i.e., finite energy). Spectral coefficients are obtained by using the Fast Fourier Transform (FFT) of the data and extracting the magnitude square of the coefficients at the location of interest, as well as the spectral location. This technique correlates spectral coefficients of signals with those obtained from selected templates.

This thesis consists of five chapters. Chapter I introduces the topic. Chapter II explains briefly wavelet analysis, the processing of the wavelet transform output, and the spectral cross-correlation technique. Chapter III explains the signal preconditioning. Chapter IV details the processing results and Chapter V presents conclusions and recommendations for future studies.

II. TRANSIENT SIGNAL ANALYSIS

A. WAVELET TRANSFORM (WT)

The Wavelet Transform (WT) is an alternative technique to the classical Short Time Fourier Transform (STFT) (i.e., the Gabor Transform [1]) which is used for the time-frequency analysis of non-stationary signals [2]. The STFT uses a single fixed analysis window, while the wavelet transform uses various analysis windows in the time domain. The wavelet transform bandwidth is inversely proportional to the width of the time window. Hence, the more narrow the wavelet function window width, the higher the center frequency is and the wider the bandwidth is. This is the reason why the WT is known as "constant Q" filtering [3]. The wavelet transform uses dilations and translations of a basis function known as the mother wavelet. The family derived from this basis function is generally of the form:

$$\psi_{ab}(t) = \frac{1}{\sqrt{a}}\psi\left(\frac{t-b}{a}\right), \tag{1}$$

where ψ is the mother wavelet, a is the scaling parameter, and b is the shifting or translation parameter. We numbered the octaves such that as the frequency increases the octave increases too. The constant $1/\sqrt{a}$ is used for energy normalization. The family of the basis functions include short duration/high frequency functions and long duration/low frequency functions. The dilations and compression of the wavelet function $\psi(t)$ enable the tiling of the time-frequency plane, as shown in Figure 1.

1. The Continuous Wavelet Transform

The Continuous Wavelet Transform (CWT) can be defined as:

$$CWT_x(a,b) = \frac{1}{\sqrt{a}}\int_{-\infty}^{\infty}\psi_{ab}(t)x(t)dt\,, \tag{2}$$

where $\psi_{ab}(t)$ is given by Equation (1).

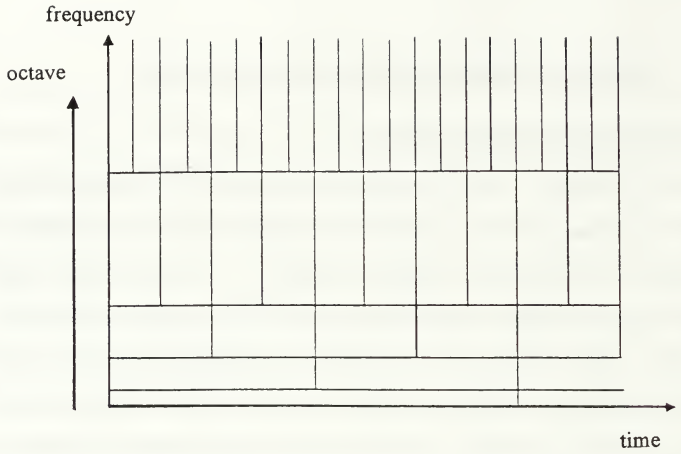

Figure 1: Tiling of the time-frequency plane.

A function $\psi(t)$ can be defined as a mother wavelet only if it is oscillatory, decays to zero at the end points, and has a zero mean [4]. The inverse of the Wavelet Transform is given by

$$x(t) = \frac{1}{C_\psi} \int_{-\infty}^{\infty} CWT_x(a,b)\psi_{ab}(t)\frac{dadb}{a^2}\,, \tag{3}$$

where C_ψ is given by

$$C_\psi = \int_0^\infty \frac{|\psi(\Omega)|^2}{\Omega} d\Omega\,, \tag{4}$$

and $\psi(\Omega)$ is the Fourier transform of $\psi(t)$. Equation (3) is valid only if $\psi_{ab}(t)$ is an admissible wavelet function which requires that $C_\psi < \infty$. This implies that $\psi_{ab}(t)$ has a zero mean. The function $\psi_{ab}(t)$ has compact support, hence it acts as the impulse response of a bandpass filter that decays very fast to zero [2].

2. The Discrete Wavelet Transform

From Equation (1), the Discrete Wavelet Transform (DWT) can be obtained by sampling the parameters a, b at discrete values which are given as

$$a \;=\; a_0^{-j}\,,$$

$$b = kb_0a_0^{-j}, \tag{5}$$

where j is the octave number, k is the sample index, $j, k \in Z$ and a_0, b_0 are pre-selected constants. We can express the discrete wavelet functions as

$$\psi_{jk}(t) = a_0^{j/2}\psi(a_0^j t - kb_0), \tag{6}$$

where $j,\ k \in Z$. The signal can be expressed as a function of this wavelet basis:

$$x(t) = \sum_j \sum_k d_{jk}\psi_{jk}(t), \tag{7}$$

where d_{jk} is the wavelet coefficient defined by:

$$\begin{aligned} d_{jk} &= \langle x(t),\ \psi_{jk}(t)\rangle \\ &= a_0^{j/2}\int_{-\infty}^{\infty} x(t)\psi^*(a_0^j t - kb_0). \end{aligned} \tag{8}$$

Under specific conditions detailed in [5], the set of $\psi_{jk}(t)$ is considered as an orthonormal set of basis for $L^2(R)$. Therefore, any function $x(t)$ in $L^2(R)$ can be represented as in Equation (7).

The uncertainty principal states that, for a given transform pair, $x(t) \leftrightarrow X(\omega)$, the inequality below holds

$$\sigma_t\sigma_\omega \geq \frac{1}{2}, \tag{9}$$

where σ_t and σ_ω are defined as [4]:

$$\sigma_t^2 = \frac{\int t^2|x(t)|^2dt}{\int |x(t)|^2dt},\ \sigma_\omega^2 = \frac{\int \omega^2|X(\omega)|^2d\omega}{\int |X(\omega)|^2d\omega}. \tag{10}$$

We note the integration equation limits $\pm\infty$ are suppressed. As seen from Equation (9), there is a lower bound for the product $\sigma_t\sigma_\omega$, hence if the signal is short in time, it will be wide in frequency. This means that we cannot find a wavelet function or Fourier basis that has an arbitrary time width and frequency bandwidth, i.e., even

for the wavelet transform analysis the time localization is a function of the frequency resolution. Accordingly, the high octave corresponds to a narrower wavelet with better time resolution than at a lower octave.

3. Multiresolution Signal Analysis

a. Multiresolution Spaces

Multiresolution analysis consists of a sequence of closed subspaces [10]

$$\cdots V_{-2} \subset V_{-1} \subset V_0 \subset V_1 \subset V_2 \cdots \tag{11}$$

that have the following properties [6]

- Completeness:

$$\cap V_j = \{0\}\,, \quad \cup V_j = L^2(R) \qquad j \in Z\,, \tag{12}$$

where $\cap$ is the intersection of subspaces and $\cup$ is the union of subspaces.

- Scaling Property:

$$x(t) \in V_j \;\leftrightarrow\; x(2t) \;\in V_{j+1}\,. \tag{13}$$

- Existence of Basis: A scaling function $\phi \in V_j$ exists such that the set

$$\left\{\phi_{jk}(t) = 2^{j/2}\phi(2^j t - k)\right\}\,, \qquad \forall j \in Z \tag{14}$$

forms an orthonormal basis for V_j. Equation (11) is demonstrated via the Venn diagram in Figure 2, as the basic idea of multiresolution analysis is that of successive approximations. An equivalent way of representing $L^2(R)$ is shown in Figure 3.

The space W_j, obtained for octave j, defined to be the orthogonal complement of the space V_j with respect to V_{j+1}, can be written as

$$V_j = V_{j-1} \oplus W_{j-1} \tag{15}$$

$$V_{j-1} \perp W_{j-1}\,, \tag{16}$$

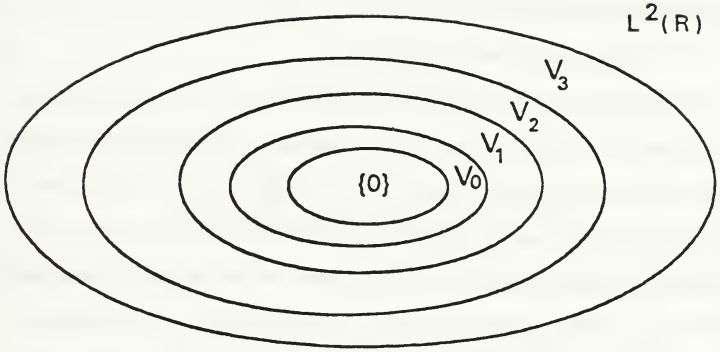

Figure 2: Equation (11) illustrated via a Venn diagram [7].

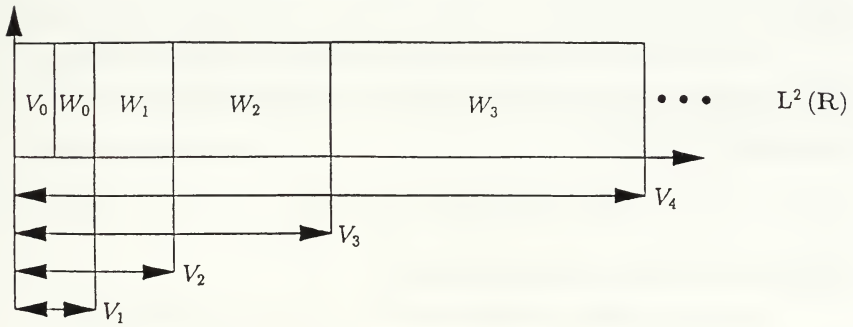

Figure 3: Multiresolution representation of $L^2(R)$ [8].

where the symbol, $\oplus$, stands for the direct sum, which means that each element of V_{j+1} can be written as the sum of the elements of V_j and W_j. Thus, W_j contains the "detail" necessary to go from V_j to V_{j+1}.

b. Scaling Functions and Wavelets

The scaling function $\phi_{jk}(t)$ used in Equation (14) is a lowpass function because it is used to go from a higher octave number to a lower octave number. It spans the coarse approximation space V_j. The wavelet function $\psi_{jk}(t)$ given in Equation (6), which for all values of k, spans the difference information space W_j, can be considered as a highpass function. Scaling and wavelet functions can represent any signal in V_{j+1}. Scaling a wavelet simply means stretching (or compressing) it. As per Equations (6) and (14), $\{\psi_{jk}(t)\}$ and $\{\phi_{jk}(t)\}$ are sets of translations of the dilated functions $\psi_j(t)$ and $\phi_j(t)$, where the scale factor is denoted by the letter j. When $j > 0$, $\phi_{jk}(t)$ compresses and V_j stretches accordingly, which results in finer details. When $j < 0$, $\phi_{jk}(t)$ stretches and V_j compresses, which results in coarser details.

Let $\phi(t)$, as used in Equation (14), be the scaling function, then its translation $\phi(t-k)$ spans V_0. The scaling function $\phi(t)$ can be written as a linear combination of the translations of $\phi(2t)$ as

$$\phi(t) = \sum_k h_0(k)\phi(2t-k)\,, \quad k \in Z\,, \tag{17}$$

where $h_0(k)$ are the scaling function coefficients.

Let $\psi(t)$, as defined by Equation (6), be an element of the subspace W_0. W_0 itself is a subspace of V_1 spanned by $\phi(2t)$. Hence, $\psi(t)$ can be written as the linear combination of the translation of $\phi(2t)$ as

$$\psi(t) = \sum_k h_1(k)\phi(2t-k)\,, \quad k \in Z\,, \tag{18}$$

where the $h_1(k)$ are the wavelet coefficients.

Since $\phi(t)$ and $\psi(t)$ span two orthogonal spaces, $h_0(k)$ and $h_1(k)$ should be orthogonal. Hence, orthogonality of V_0 and W_0 can be accomplished by requiring that

$$\langle h_0(k),\ h_1(k)\rangle = 0\,. \tag{19}$$

Any $x(t)$ in $L^2(R)$ can be represented as

$$x(t) = \sum_{k=-\infty}^{\infty} a_k\phi_k(t) + \sum_{j=1}^{\infty}\sum_{k=-\infty}^{\infty} d_{jk}\psi_{jk}(t)\,, \tag{20}$$

with a_k and d_{jk} being discrete wavelet transform coefficients which are defined by

$$\begin{aligned} a_k &= \langle x(t)\,,\phi_k(t)\rangle = \int_{-\infty}^{\infty} x(t)\phi_k(t)dt \\ d_{jk} &= \langle x(t)\,,\psi_k(t)\rangle = \int_{-\infty}^{\infty} x(t)\psi_{jk}(t)dt\,, \end{aligned} \tag{21}$$

where $\phi_k(t)$ and $\psi_{jk}(t)$ are real functions. According to Equation (20), any function in $L^2(R)$ can be written as a linear combination of the scaling function at a fixed scale plus a linear combination of wavelet functions at a higher scale. For more details regarding the properties of wavelet transform, see Payal [8].

A typical wavelet set up is shown in Figure 4. This is according to the following equations [9]:

$$a_{jk} = \sum_m \overline{h}_0(m-2k)a_{j+1,m} \tag{22}$$

$$d_{jk} = \sum_m \overline{h}_1(m-2k)a_{j+1,m} \tag{23}$$

where $\overline{h}_0(k)$ and $\overline{h}_1(k)$ are given by

$$\begin{aligned} \overline{h}_0(k) &= h_0(-k) \\ \overline{h}_1(k) &= h_1(-k)\,. \end{aligned} \tag{24}$$

where $\overline{h}_0(k)$ and $\overline{h}_1(k)$ are the impulse response time reversals. The wavelet implementation for three levels is shown in Figure 5. The notation LP stands for lowpass FIR filter whose weights are $h_0(-k)$, and HP stands for highpass FIR filter whose weights are $h_1(-k)$.

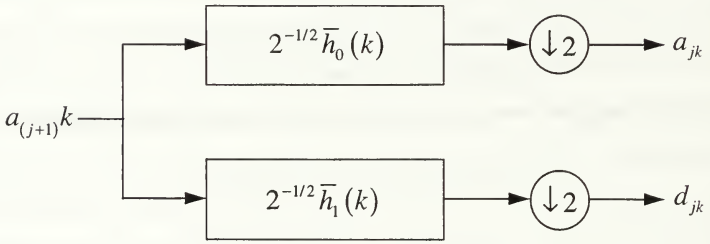

Figure 4: One stage of multiresolution signal decomposition.

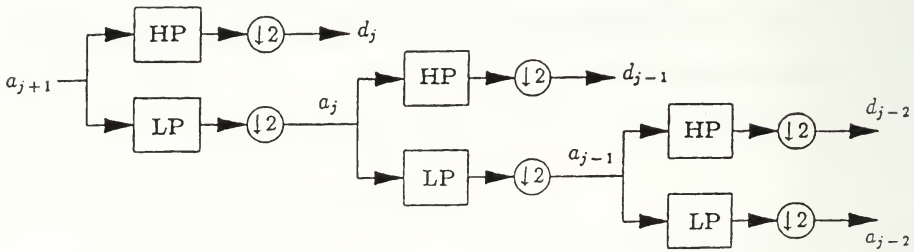

Figure 5: Three level multiresolution analysis.

4. Processing of Wavelet Transform Output

a. Reduced Set Representation

The method introduced previously in the preprocessing of the wavelet transform output [8] is applied in this thesis, where the extrema of the wavelet coefficient are used to identify the original signal. The wavelet coefficients are replaced by their extrema and the Euclidian distance between these extrema is measured. The computer programs related to preprocessing, wavelet processing, and cross-correlation of the spectral coefficient are presented in Appendix A.

b. Ranking and Matching Algorithm

Once the peaks, which are the extremal values of the wavelet coefficients, are provided for the templates and the signals, they are ranked by their amplitudes. Then, matching the ranked peaks to form pairs, the peak with the highest rank in one set is matched to the peak with the highest rank in the other. Finally, the next in rank is matched by the next of the other set and so on.

c. Distance Measure

The distance measure, which was introduced in 1992 by Aware, Inc., is used in a modified form for the classification of signals in this thesis work. The Euclidian distance is defined as

$$d(a^j, b^j) = \sum_{(k,\ell) \text{ are locations of the matched peaks}} \left[W^j_{k,\ell} \left(a^j_k - b^j_\ell \right)^2 \right]^{1/2} \tag{25}$$

where a^j and b^j are wavelet maxima at scale j. $W^j_{k,\ell}$ is the weighting factor at scale j for the relative distance between the similar coordinates of the matched peaks, and a^j_k and b^j_k are the values a^j and b^j at momentary location k and ℓ. The weighting factor $W^j_{k,\ell}$ is defined as

$$W^j_{k,\ell} = \begin{cases} |n^j_k - n^j_k| & ; \quad k \neq \ell \\ 1 & ; \quad k = \ell \end{cases} . \tag{26}$$

B. SPECTRAL CROSS-CORRELATION

1. Introduction

Spectral correlation analysis provides a useful tool for the classification of transient signals. These signals (data) are functions of time and are given in digitized form. Spectral coefficients are obtained by applying the Fast Fourier Transform (FFT) to the data, and extracting the magnitude squared of the coefficients at the location of interest, as well as the spectral location [10].

Each of the digitized transient signal is 4096 data points long. When the spectral coefficients were plotted it was found that all data of interest was in the first 32 spectral locations. The plots were inspected to confirm that none of the remaining locations contained valuable data. To be considered valuable, the spectral density must exceed 10% of the peak value. The resultant is plotted for all data sets of all transmitters (see Figure 6). We note the relevant information always exists only in the low frequency region.

For this analysis, an averaged template for each signals set is obtained by averaging all spectral densities of a given transmitter (see Figure 7). Then the spectral coefficients of all signals of interest are obtained. These spectral coefficients are examined to determine whether or not this signal belongs to the set which created the template. The first step in the processing chain is to find the power in the first 32 spectral locations given by

$$A(k) = \left| \sum_{n=0}^{4095} a_s(n) e^{-j2\pi \frac{kn}{N}} \right|^2 \quad \text{for} \quad k = 0, 1, \cdots, 31 ; \tag{27}$$

where $a_s(n)$ is the discrete time signal of the data (signal) and N is the data equal to length 4096. The spectral coefficients are computed for all templates and signals of interest. The degree of similarity between two vectors $A_{\text{template}}(k)$ and $A_{\text{signal}}(k)$ can be determined by correlating the vectors under consideration.

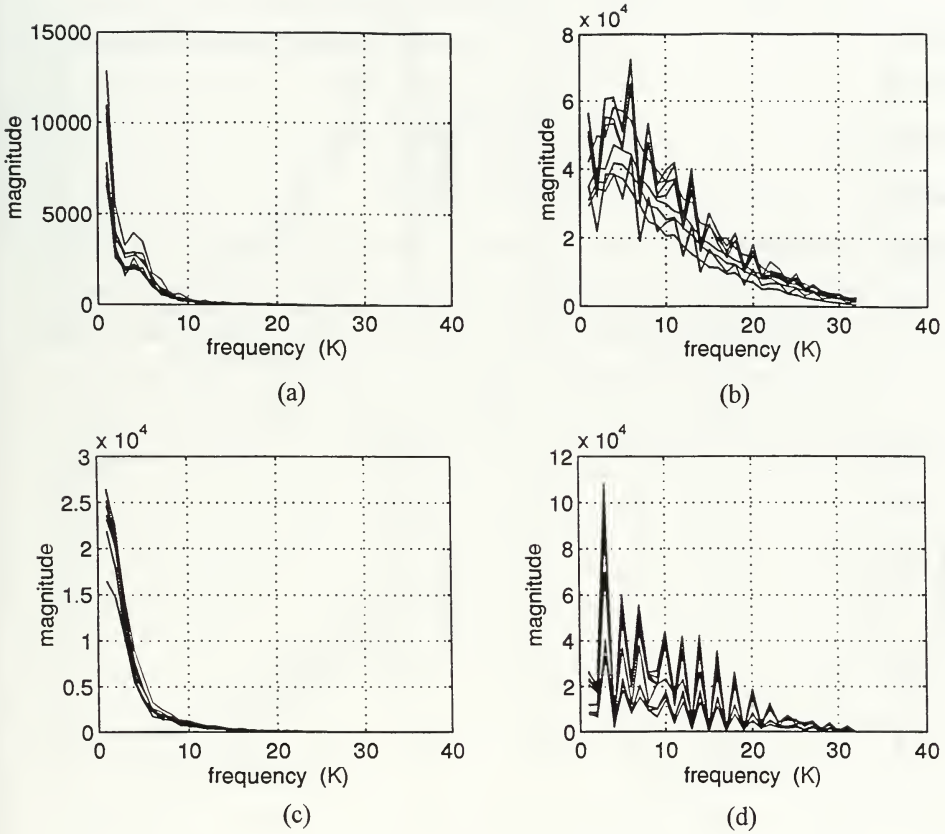

Figure 6: Superimposed spectra for transients contained in (a) Transmitter 1, (b) Transmitter 2, (c) Transmitter 3, (d) Transmitter 4.

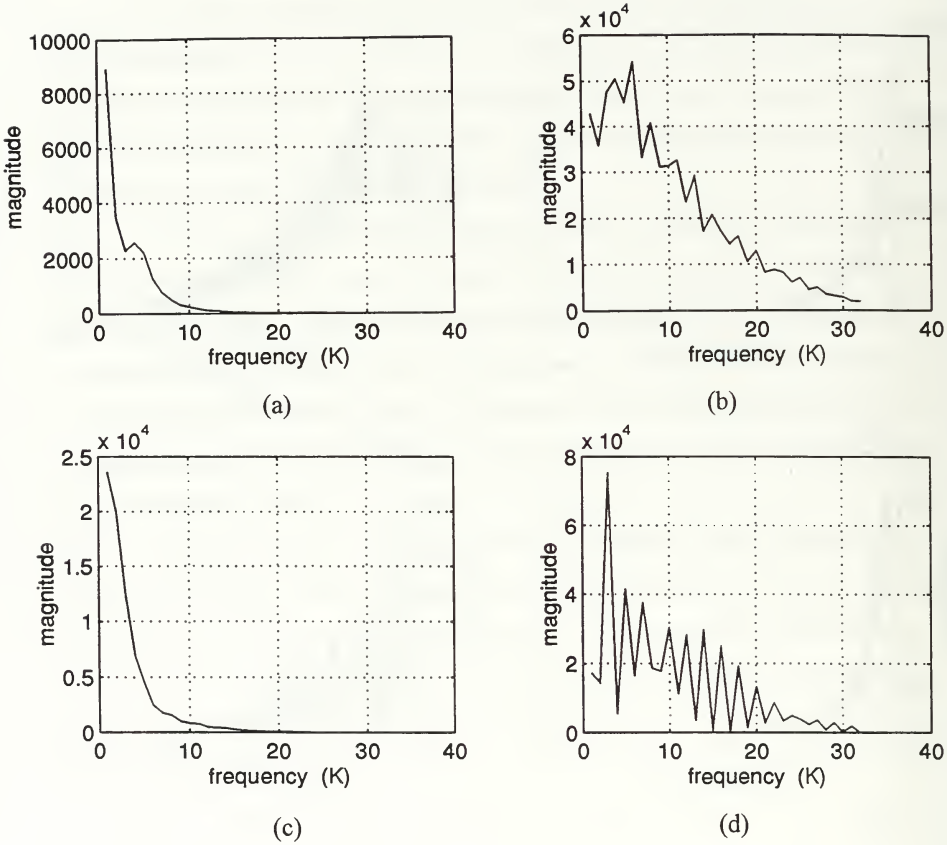

Figure 7: Averaged spectral plot for the four sets of transients: (a) average template for TR1, (b) average template for TR2, (c) average template for TR3, (d) average template for TR4.

2. Normalized Cross-Correlation Coefficient

Prior to cross-correlating the two vectors $A_t(k)$ and $A_s(k)$, the mean value of each vector (i.e., template and signal) is removed. The coefficient obtained is the normalized correlation coefficient given by

$$\rho_{xy} = \frac{\sum_{k=0}^{31} A_t(k) A_s(k)}{\sqrt{\sum_{k=0}^{31} |A_t(k)|^2 \sum_{k=0}^{31} |A_s(k)|^2}}. \tag{28}$$

Thus, the range of this normalization will keep the cross-correlation coefficient between -1 and $+1$ and will aid in an automated decision. If ρ, the normalized cross correlation coefficient is one it indicates that the two signals are identical (even if they are scaled versions of each other). A high value implies that the template and the signal are from the same set, while a small value implies that they belong to different sets.

III. SIGNAL PRECONDITIONING

A. TURN-ON AND TURN-OFF SIGNALS OF PUSH-TO-TALK RADIOS

The data was collected and recorded by the Naval Security Group Activity, Charleston, SC. Nine samples of turn-on and turn-off transients of four different transmitters were collected. The recordings from each transmitter are numbered from one to nine. Figure 8 shows the first turn-on transient from each transmitter. The signals were collected by an antenna, processed with a radio receiver of a carrier frequency equal to 138.525 MHz, filtered with a 1 MHz bandwidth filter (BW), and digitized with a sampling frequency of 5 MHz at a center frequency of 1.075 MHz. Figure 9 shows the first turn-off transients from each transmitter. Significant information for the identification can be found in the envelope, which contains low frequency components. Wavelet transforms are not practical for the analysis of low frequency, but are well-suited for short duration phenomena. Accordingly, the data is transformed into a form suitable for wavelet transforms. This is done in the preprocessing phase. It should also be noted that the signal-to-noise ratios of the signal recorded are not known, and a denoising process would enhance the identification performance. All the radios are Motorola radios. Each is identified by its name, number, and model as tabulated in Table 1.

B. PREPROCESSING PHASE

The signals go through four stages in the preprocessing phase. The four stages are: taking the envelope, filtering, differentiating, and a final filtering. Before taking the envelope, the D.C. term is removed. The first filter, which filters the envelope, is a 100-point boxcar averager. The second filter, which is used after differentiation, is a 50-point boxcar averager. The filters sizes were experimentally determined [10]. The

processing of the data deals only with the turn-on transient because the turn-off transient does not permit identification. Figure 10 shows the first preprocessed signal of each of the four transmitters. All of the four final pulse-shaped signal waveforms seem to be suitable for wavelet transform analysis.

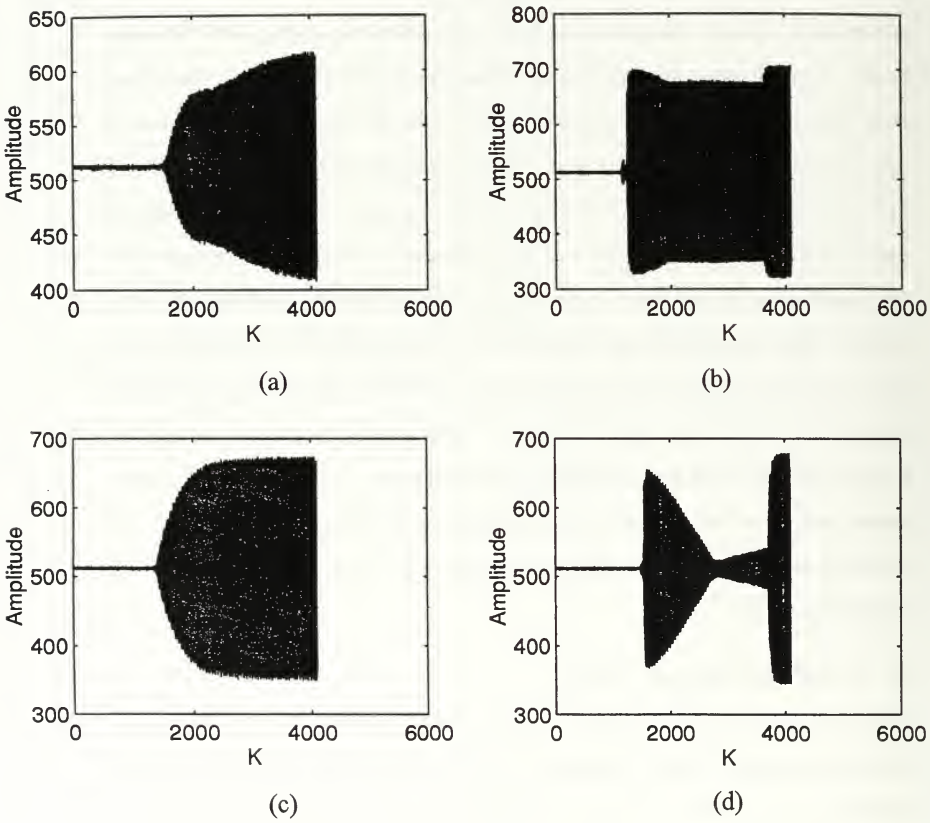

Figure 8: Turn-on signal samples from four different transmitters: (a) Signal 1 from Transmitter 1, (b) Signal 1 from Transmitter 2, (c) Signal 1 from Transmitter 3, (d) Signal 1 from Transmitter 4.

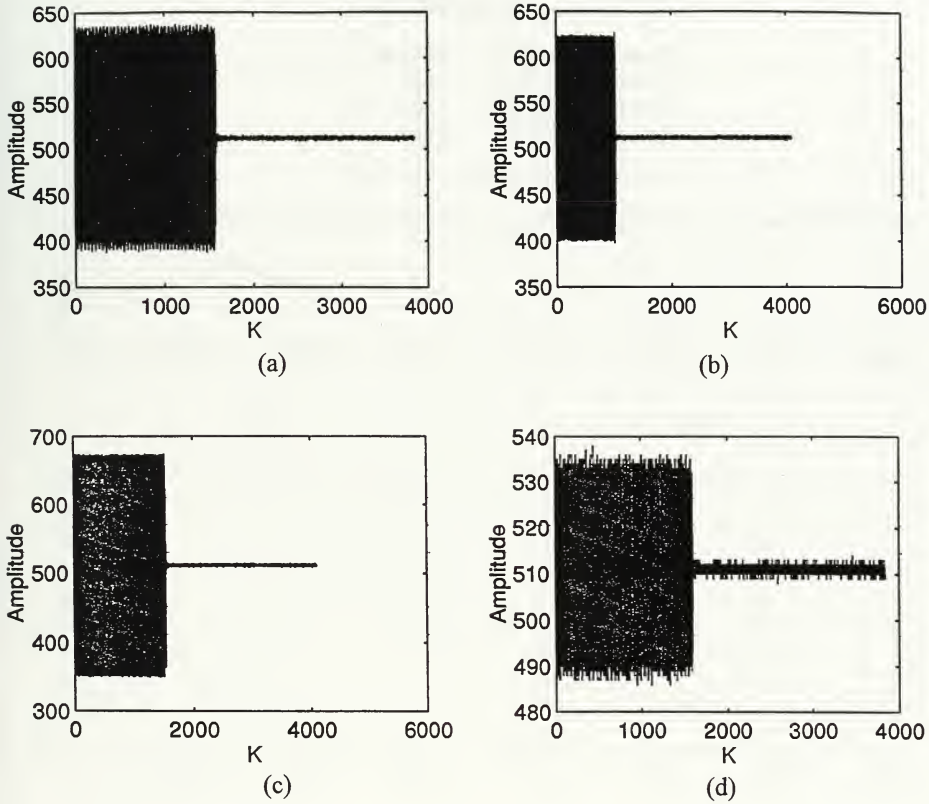

Figure 9: Turn-off signal samples from four different transmitters: (a) Signal 1 from Transmitter 1, (b) Signal 1 from Transmitter 2, (c) Signal 1 from Transmitter 3, (d) Signal 1 from Transmitter 4.

Table 1: Name and Model of the Four Transmitters

Radio	Model
Transmitter 1 (Tr1)	Maxtrac
Transmitter 2 (Tr2)	Saber
Transmitter 3 (Tr3)	HT440
Transmitter 4 (Tr4)	Saber

Note that Tr2 and Tr4 are different radios, but they are of the same model.

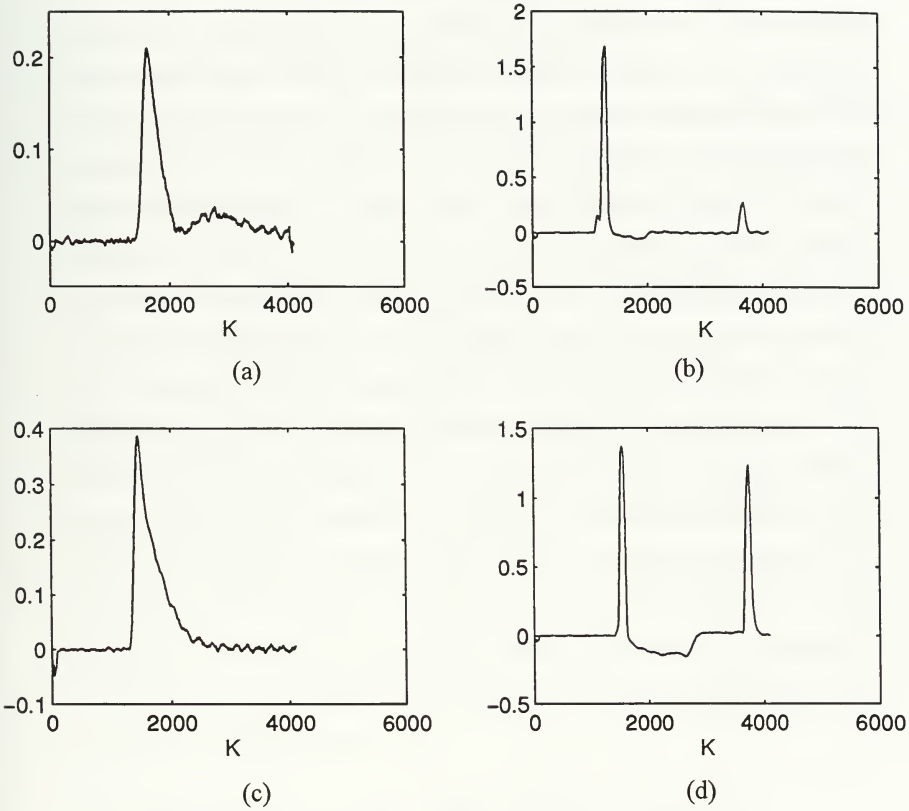

Figure 10: Preprocessed signal samples from four different transmitters: (a) Signal 1 from Transmitter 1, (b) Signal 1 from Transmitter 2, (c) Signal 1 from Transmitter 3, (d) Signal 1 from Transmitter 4.

IV. PROCESSING RESULTS

A. WAVELET TRANSFORM TECHNIQUE

The data was re-processed by the wavelet transform technique to validate the integrity of the acquired data and the results of the previous work [8]. The distance measure algorithm is applied to classify or identify the signals (i.e., which signal belongs to which transmitter). The eighth-order Daubechies wavelet function is used to compute the wavelet transform of the processed signals [8]. The signal-to-noise ratios of all the signals are computed. The average SNRs are 34.8 dB, 41.1 dB, 40.6 dB, and 34.6 dB for set 1, set 2, set 3, and set 4, respectively. Scale 11 appears to be the best scale for the data at hand [8]. Ten noisy realizations are generated using white Gaussian noise. The noise is added to the set to increase the noise level (i.e., to decrease the signal-to-noise ratio). The probability of identification versus different SNRs' plots for the wavelet transform technique are obtained and shown in Figure 11 for the four transmitters. It can be seen that the WT distance algorithm is able to classify the four signal sets accurately. Also, good identification results are achieved at low signal to noise ratios. For example, it is found that for transmitter 1 a 1.0 probability of identification is achieved at 16 dB, which is considered a reliable identification. For transmitters 2, 3, and 4, it is found that the WT distance algorithm is reliable above the SNR levels of 28 dB, 23 dB, and 21 dB, respectively. These results are identical to those obtained in [8].

B. NORMALIZED WAVELET TRANSFORM TECHNIQUE

In this technique we scaled the signals and the templates of each transmitter to normalize the energy of the signals and the templates. The normalization is done by dividing the data vector (*mdmyi*) by the square root of its sum of the square values

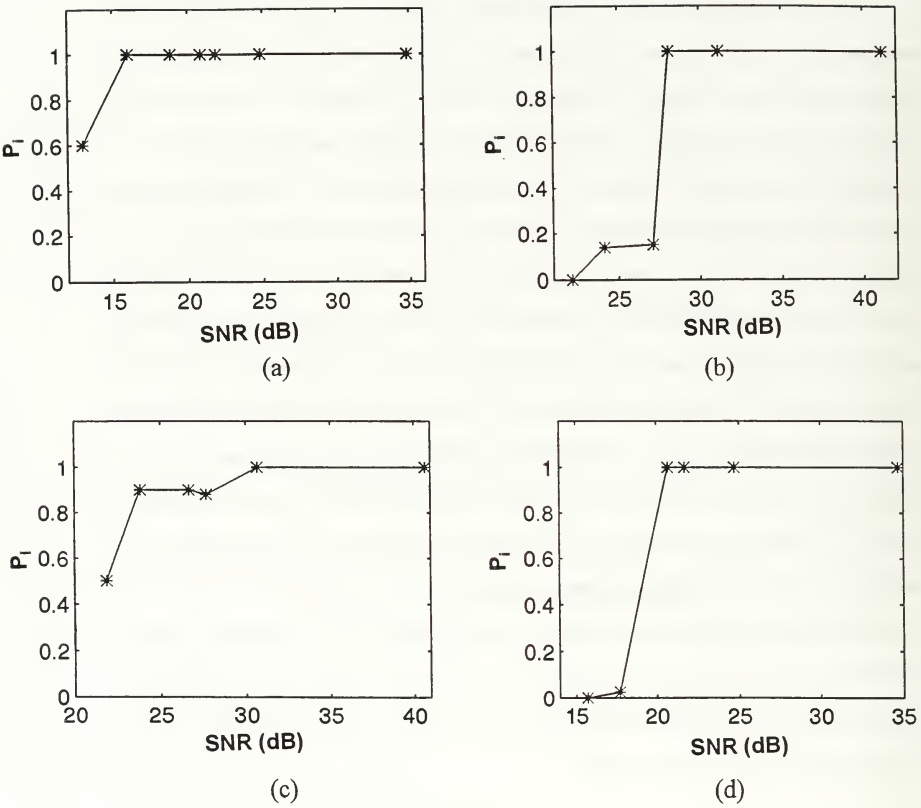

Figure 11: Probability of identification (P_i) of the signals using the WT approach: (a) P_i of signals from Tr1, (b) P_i of signals from Tr2, (c) P_i of signals from Tr3, (d) P_i of signals from Tr4.

as shown below

$$mdmyi_\ell(n) = \frac{mdmyi_\ell(n)}{\sqrt{\sum_n mdmyi_\ell(n)^2}}, \quad \text{for} \quad \begin{matrix} i = 1, \cdots, 9 \\ \ell = 1, \cdots, 4 \end{matrix} \tag{29}$$

where $mdmyi_\ell(n)$ is the i^{th} pre-processed signal of the ℓ^{th} transmitter. The chosen templates are normalized similarly. The wavelet transform is computed and the WT distance algorithm is applied. Ten realizations are conducted using different randomly generated noise for different SNRs. The results show that some of the WT distance between the template and its own set gets larger, while the WT distances to the other sets get smaller. This will not lead to a firm classification since a good and reliable classification can only be achieved if the distance between the template and its own set is small and its distance to the other sets are large. The results of using the normalized wavelet transform is shown in Figure 12. We see shows that this method performs better than the wavelet transform for two sets of signals and worse for the other two sets. For example, in the wavelet transform method a high probability of identification of transmitter 1 can be achieved at an SNR of 16 dB. While using the normalized wavelet transform method, a high probability of identification can be achieved at 21.8 dB. Therefore, a degradation of 5.8 dB seems to occur. These results reveal that the normalized version of the wavelet transform does not perform better than that without normalization. This may be due to the negative values in some of transmitter 1 pre-processed signals. The negative values contribute to the square root of the sum of the squares. Signal 1 is selected as a template for the first set and, as shown in Figure 13, does not have large negative values. For illustration, Figure 13(b) shows signal 9 from set 1, where the negative spike can be observed. If we remove the negative spikes from the signals, the distance between the template and its own set become smaller and

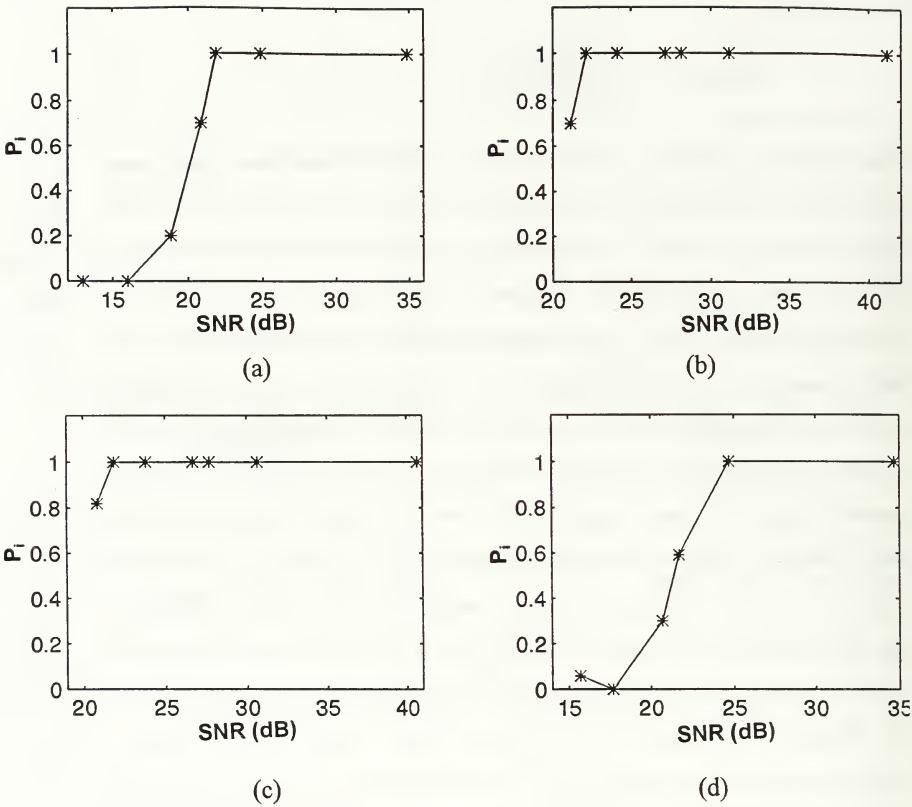

Figure 12: Probability of identification (P_i) of the signals using normalized wavelet approach: (a) P_i of signal from Tr1, (b) P_i of signal from Tr2, (c) P_i of signal from Tr3, (d) P_i of signal from Tr4.

distances to other sets become larger, indicating that the negative spikes cause part of the performance degradation.

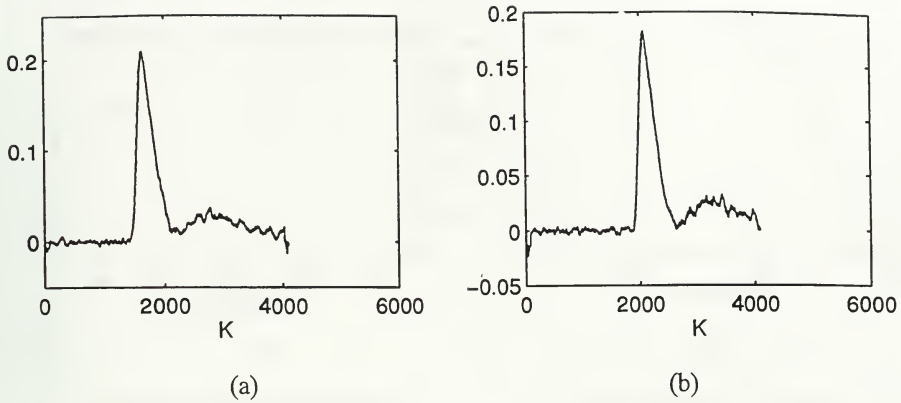

Figure 13: Plots of preprocessed signals 1 and 9 from Transmitter 1: (a) signal 1 from Tr1, (b) signal 9 from Tr1.

C. SPECTRAL CROSS-CORRELATION TECHNIQUE

The aim of this approach is to utilize an automated method to introduce a robust identifier. The normalized cross correlation is bounded by $+1$ and -1. A "1" signifies that the two signals under consideration are 100% alike while "0" signifies no likeness. The normalized cross-correlation is independent of the signal amplitude. It measures the waveform similarities of two signals. We take the FFT of the preprocessed data, extract the magnitude squared of the coefficients, and retain the spectral coefficients with non-zero values. The dominant spectral coefficients are available from the first 32 spectral locations to capture the relevant information. The four averaged templates (Figure 7), chosen for their similarity within each set, are cross-correlated with the four signal sets. For the different SNRs, ten realizations are generated using independent noise. The processing results using this technique are shown in Figure 14 by plotting probability of identification (P_i) versus SNR.

As we can see from the plots, the spectral correlation technique gives a better result than those based on the normalized and the non-normalized wavelet transform

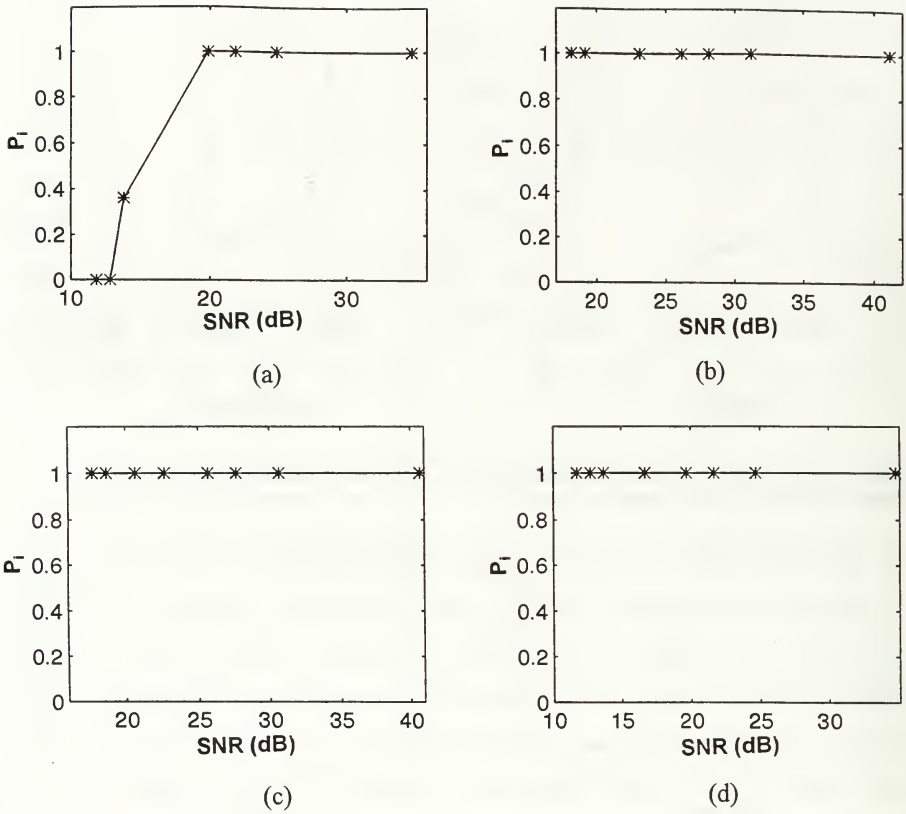

Figure 14: Probability of identification (P_i) of the signals using spectral cross-correlation approach: (a) P_i of signals from Tr1, (b) P_i of signals from Tr2, (c) P_i of signals from Tr3, (d) P_i of signals from Tr4.

(i.e., high probability of identification at lower signal-to-noise ratios) except for template 1. The similarity between the waveform of template 1 and those of the signals belonging to transmitter 3 may be the reason behind the unsatisfactory performance of template 1. This similarity more likely occurs when we add white Gaussian noise to the signals of set 3. We investigated the data leading to the ROC curve of template 1, which is shown in Figure 15.

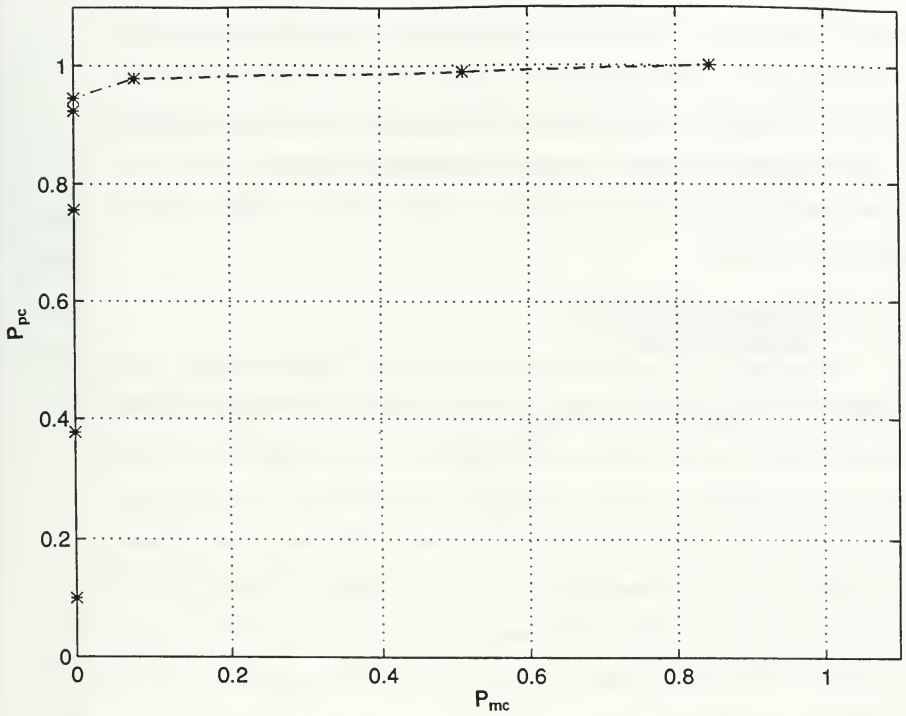

Figure 15: Performance curve for the probability of proper classification (P_{pc}) versus the probability of miss-classification (P_{mc}) of template 2 at 19.8 dB.

It was found that, to obtain a certain probability of classification, the threshold should be set to a specific value. For example, when the threshold is set to 0.98 the probability of proper classification is found to be 0.3778 with a 0 probability of misclassification. When it is required to have a high probability of proper classification as 0.9778, the probability of misclassification is 0.0778 which can be considered as an acceptable case. This investigation was done with template 1 at a

signal-to-noise ratio of 19.8 dB. The other templates are performing perfectly, as shown in Figure 14, with low SNRs of 18.1 dB, 17.6 dB, and 11.6 dB for template 2, 3, and 4, respectively. The threshold plots of the degraded signal-to-noise ratio of 10 db and 22 dB for template 1 are shown in Appendix B (Figures 18 and 19). No further analysis is performed for templates 2, 3, and 4 because template 1 failed to work below 19.957 dB.

D. PROCESSING SUMMARY

The results of the three techniques are summarized in Figures 16 and 17. From the plots it can be seen that the spectral correlation approach outperforms the other two approaches for most transmitters. It was found that, for templates 2, 3, and 4, the spectral correlation gave a high probability of identification of 1.0 at low signal-to-noise ratio up to as low as 18.1 dB, 17.6 dB, and 11.6 dB, respectively. Whereas the wavelet and the normalized wavelet gave a high probability of identification of 1.0 up to as low as 28.1 dB and 22.1 dB for template 2; 23.8 dB and 21.8 dB for template 3; 20.6 dB and 24.6 dB for template 4. The spectral correlation approach works well for templates 2, 3, and 4.

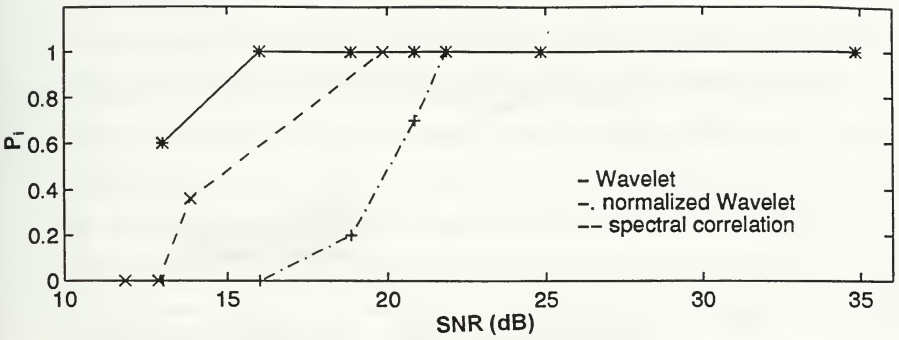

(a)

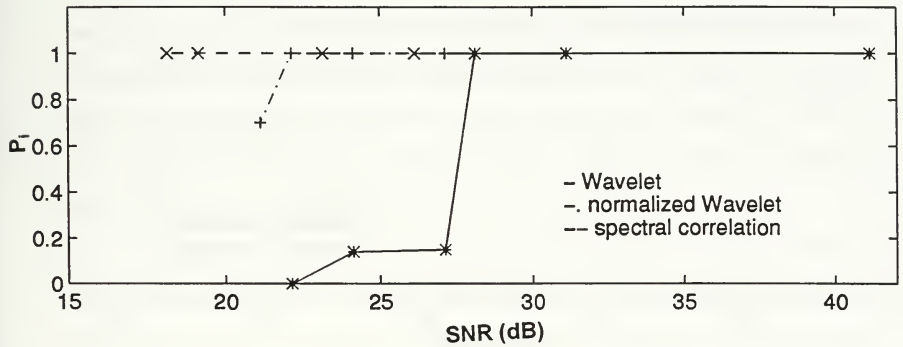

(b)

Figure 16: Probability of identification (P_i) plots versus signal-to-noise ratio (SNR in dB) for the three techniques, (a) P_i of signals from TR1, (b) P_i of signals from TR2.

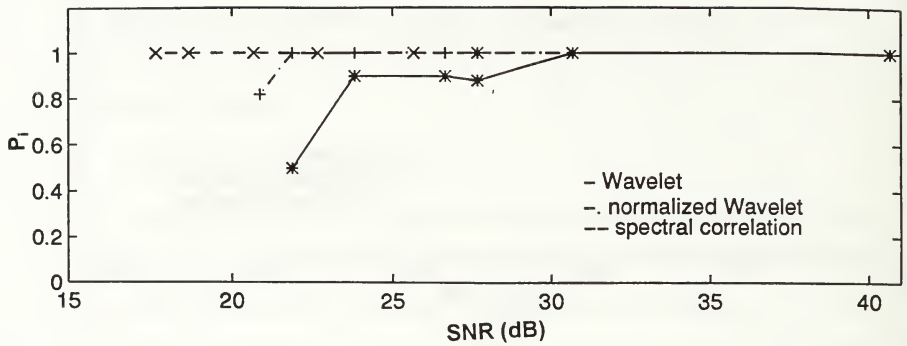

(a)

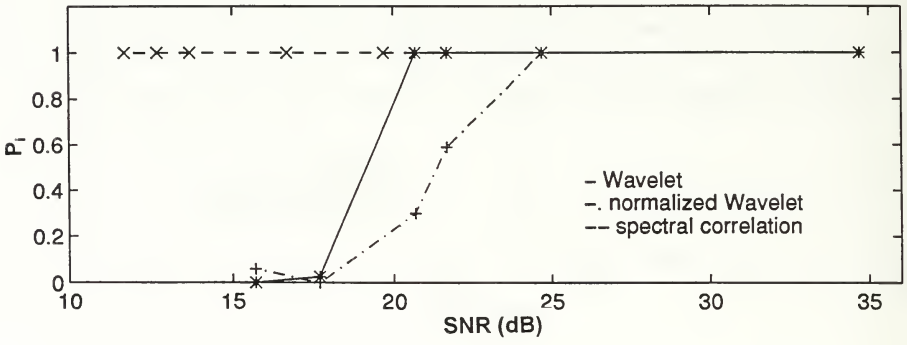

(b)

Figure 17: Probability of identification (P_i) plots versus signal-to-noise ratio (SNR in dB) for the three techniques, (a) P_i of signals from TR3, (b) P_i of signals from TR4.

V. CONCLUSIONS AND RECOMMENDATIONS

A. CLASSIFICATIONS OF PUSH-TO-TALK COMMUNICATIONS SIGNALS

This thesis investigated the application of the wavelet transform and spectral correlation to identify several types of push-to-talk transmitters. The data provided for this work was turn-off/turn-on transients collected from push-to-talk radios. Nine transmissions from four different transmitters were used in the identification part of this thesis. The turn-on transients are unique for each transmitter. Results show that the spectral cross-correlation method out-performs the other two techniques.

B. RECOMMENDATION FOR FUTURE STUDIES

The spectral correlation approach introduced in Chapter IV, Section C gave the most promising results in classifying/identifying the four signal sets. An attempt was made to select a robust template from each signal set for wavelet processing by averaging the two dominant signals in each set with respect to the signal amplitude. However, poor results were observed. Further studies are recommended to find a robust template selection for wavelet processing to make the decision statistically more reliable.

No attempt was made to use information from more than one scale simultaneously. This might make the identification process more robust, so this subject is a goal for future study. Finally, other wavelet functions could be investigated for use in the identification process.

APPENDIX A

This program is to run wt signal to transform the data into a pulse shape form. It is also to map them and select the first four signals as templates.

```
%    DATARUN1.M
% Must load data from thesis1 subdirectory,
%   cd to ../thesis, then run datarun1

% written by: abdulla
% last mod: 02/28/96

Ys=[]; %define strings 'y -yyy'
Xs=[];



for n=1:4
   Xs=[Xs, 'x'];
   Ys=[Ys, 'y'];
   disp(' ')
   disp(['Outer loop: ',Xs])

   for m=1:9
     S1=[Xs, int2str(m)];
     S2=[Ys, int2str(m)];
     disp(['   Inner loop: ',S1])
     eval(['w',S1,'=mdm',S2,';']);
     eval(['a',S1,'=map(w',S1,',8);']);
     if m==1
        eval(['at',int2str(n),'=a',S1,';']);
     end
   end
end
```

The purpose of this program is to compute the distance measurement between the signals and the four templates.

```
% DATARUN2.M
% THIS PROGRAM FIND THE DISTANCE BETWEEN THE SIGNALS AND THE TEMPLATES

% written by Abdulla M.
% last modified 02/28/96


 Xs=[]

    for n=1:4
        Xs=[Xs, 'x'];
        for m=1:9
            eval(['dx',int2str(n),'(',int2str(m),',:)=distance2(a',Xs,int2str(m),...
            ',at4',')']) % template variables are at1, at2, at3, at4.
         end
    end
```

This program transforms all noisy data into a pulse shape.

```
%               CONV1.M
% Must load datagen from thesis1 subdirectory,
%   cd to ../thesis, then run datarun1
% written by: abdulla, Abdulla M.
% last mod: 05/4/96

Ys=[]; %define strings 'y -yyy'
Xs=[];



for n=1:4
   Xs=[Xs, 'x'];
   Ys=[Ys, 'y'];
   disp(' ')
   disp(['Outer loop: ',Xs])

   for m=1:9
     S1=[Xs, int2str(m)];
     S2=[Ys, int2str(m)];
     disp(['   Inner loop: ',S1])
     eval(['mdm',S2,'=wtsig(',S1,');']);
   end
end
```

```
%%                    xc.m
%%  This program computes the fft of the pre-processed signals (mdmy's) and
%%  cross correlate them with the chosen templates
%%  Written by Abdulla, Abdulla M.
%%  Last modified 06/7/96

L=4096;    % length of the vectors mdmy's 2 to the power of N
z11=tmplt1; % tmplt2, tmplt3, and tmplt4
z11=z11-mean(z11);

a2=mdmy1; % mdmyy1, mdmyyy1, and mdmyyyy1.
z2=abs(fft(a2,L).^2);
z22=z2(1:32);
z22=z22-mean(z22);
c1=xcorr(z11,z22,'coeff');

a3=mdmy2;
z3=abs(fft(a3,L).^2);
z33=z3(1:32);
z33=z33-mean(z33);
c2=xcorr(z11,z33,'coeff');

a4=mdmy3;
z4=abs(fft(a4,L).^2);
z44=z4(1:32);
z44=z44-mean(z44);
c3=xcorr(z11,z44,'coeff');

a5=mdmy4;
z5=abs(fft(a5,L).^2);
z55=z5(1:32);
z55=z55-mean(z55);
c4=xcorr(z11,z55,'coeff');

a6=mdmy5;
z6=abs(fft(a6,L).^2);
z66=z6(1:32);
z66=z66-mean(z66);
c5=xcorr(z11,z66,'coeff');

a7=mdmy6;
z7=abs(fft(a7,L).^2);
z77=z7(1:32);
z77=z77-mean(z77);
c6=xcorr(z11,z77,'coeff');
```

```
a8=mdmy7;
z8=abs(fft(a8,L).^2);
z88=z8(1:32);
z88=z88-mean(z88);
c7=xcorr(z11,z88,'coeff');

a9=mdmy8;
z9=abs(fft(a9,L).^2);
z99=z9(1:32);
z99=z99-mean(z99);
c8=xcorr(z11,z99,'coeff');

a10=mdmy9;
z10=abs(fft(a10,L).^2);
z1010=z10(1:32);
z1010=z1010-mean(z1010);
c9=xcorr(z11,z1010,'coeff');
```

APPENDIX B

In this appendix two plots are shown. In Figure 18 we can see that at 10 dB degradation one can set a threshold between template 1 and the other transmitters (i.e., all other signals other than transmitter 1 are not similar to template 1). In Figure 19 we can see that transmitter 3 signals are becoming similar to template 1 and starting to cross each other at 22 dB degradation.

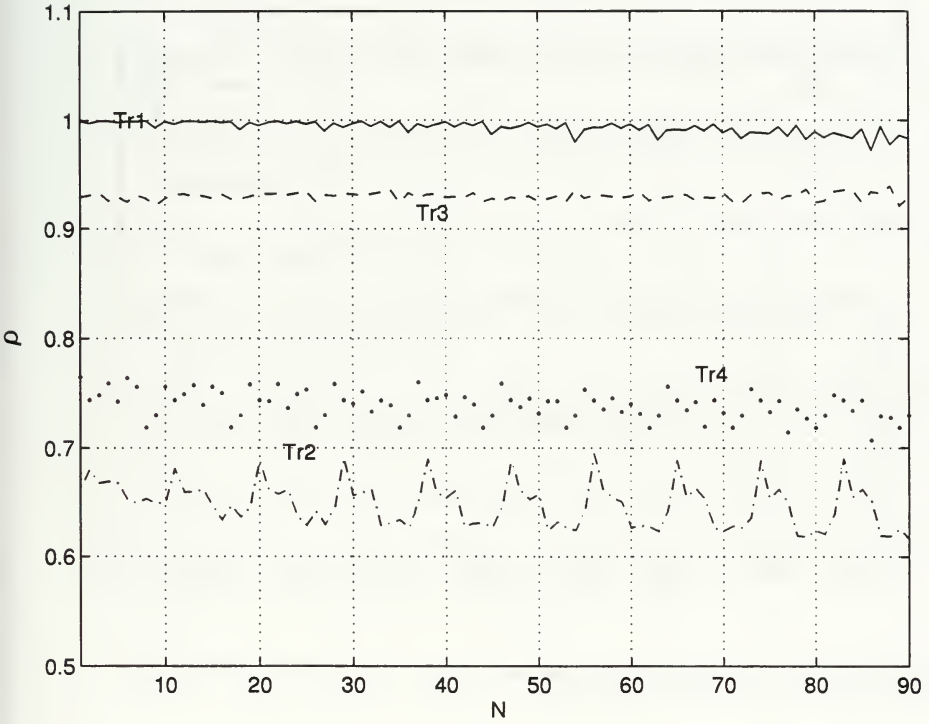

Figure 18: 10 dB degradation experimental automated threshold for template 1/set 1, set 2, set 3, and set 4.

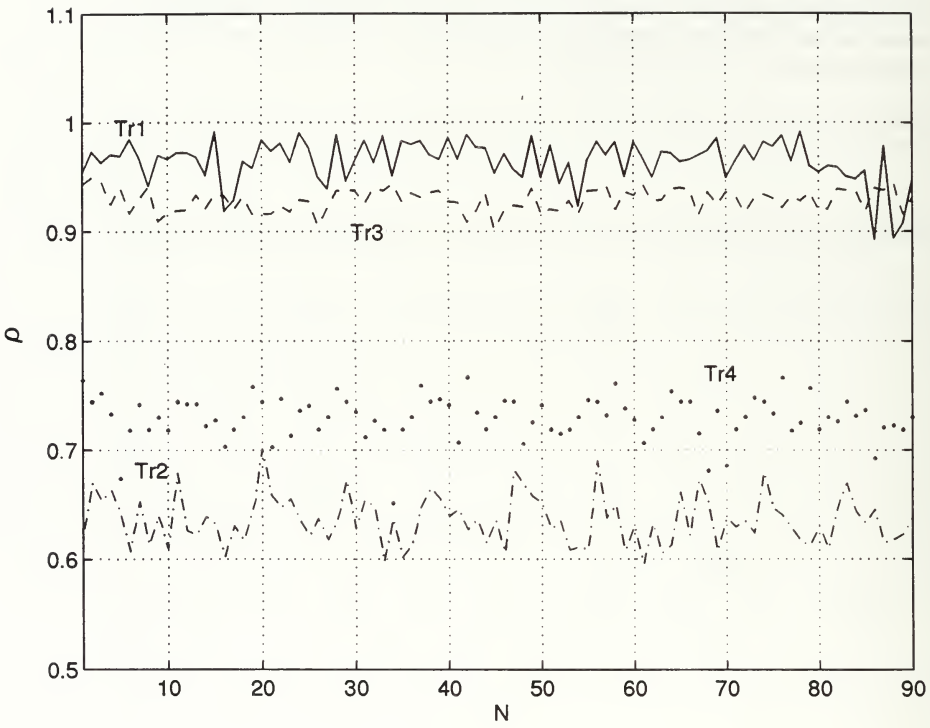

Figure 19: 22 dB degradation experimental automated threshold for template 1/set 1, set 2, set 3, and set 4.

LIST OF REFERENCES

[1] Gabor, D., "Theory of Communication," *Journal of IEEE*, Vol. 93, pp. 429–457, 1946.

[2] Akansu, A. N., and Haddad, R. A., *Multiresolution Signal Decomposition*, Academic Press, Inc., San Diego, CA, 1992.

[3] Rioul, O. and Vetterli, M., "Wavelets and Signal Processing," *IEEE SP Magazine*, pp. 14–38, October 1991.

[4] Young, R. K., *Wavelet Theory and its Applications*, Kluwer Academic Publishers, Boston, MA, 1993.

[5] Daubechies, I., "The Wavelet Transform, Time-Frequency Localization and Signal Analysis," *IEEE Transactions on Information Theory*, Vol. 36, pp. 961–1005, September 1990.

[6] Vetterli, M., and Kovacevic, J., *Wavelets and Subband Coding*, Prentice-Hall, Inc., Englewood Cliffs, NJ, 1995.

[7] Mallat, S. G., and Zhoung, S., "Complete Signal Representation with Multiscale Edges," Technical Report 483, Courant Institute of Mathematical Sciences, New York University, December 1989.

[8] Payal, Y. "Identification of Push-to-Talk Transmitters Using Wavelets," Master's Thesis, Naval Postgraduate School, Monterey, CA, 1995.

[9] Burrus, C. S., and Gopinath, R. A., "Introduction to Wavelets and Wavelet Transforms," Tutorial #1, *IEEE ICASSP '93*, Minneapolis, MN, April, 1993.

[10] Fargues, M. P., and Hippenstiel, R., "Investigation of Spectral-Based Techniques for Classification of Wideband Transient Signals," Technical Report NPSEC-93-008, Naval Postgraduate School, March 1993.

INITIAL DISTRIBUTION LIST

		No. Copies
1.	Defense Technical Information Center 8725 John J. Kingman Road, STE 0944 Ft. Belvoir, VA 22060-6218	2
2.	Dudley Knox Library Naval Postgraduate School 411 Dyer Road Monterey, CA 93943-5101	2
3.	Chairman, Code EC Department of Electrical and Computer Engineering Naval Postgraduate School Monterey, CA 93943-5121	1
4.	Professor R. Hippenstiel, Code EC/Hi Department of Electrical and Computer Engineering Naval Postgraduate School Monterey, CA 93943-5121	2
5.	Professor M. P. Fargues, Code EC/Fa Department of Electrical and Computer Engineering Naval Postgraduate School Monterey, CA 93943-5121	1
6.	Professor T. T. Ha, Code EC/Ha Department of Electrical and Computer Engineering Naval Postgraduate School Monterey, CA 93943-5121	1
7	Professor G. S. Gill, Code EC/Gl Department of Electrical and Computer Engineering Naval Postgraduate School Monterey, CA 93943-5121	1
8.	Khalil Nabil, Code EC/Hi Department of Electrical and Computer Engineering Naval Postgraduate School Monterey, CA 93943-5121	1

No. Copies

9. Dr. Mike Shieldcrout — 1
Naval Information Warfare Activity
9800 Savage Road
Ft. George Mead, MD 20755-6000

10. Abdulla Mufarrah Abdulla — 5
P.O. Box 13433
Muharraq, Bahrain
Arabian Gulf